

# Numerical Investigation of the Combined Impact of Reactor Pressure and Heating Rate on Evolution and Yields of Biomass Pyrolysis Products in Thermally Thin Regime

Pious O. Okekunle<sup>1\*</sup>, Emmanuel A. Osowade<sup>2</sup>, Joseph O. Oyekale<sup>3</sup>

1. Department of Mechanical Engineering, Faculty of Engineering and Technology,  
Ladoke Akintola University of Technology, P.M.B. 4000, Ogbomosho, Oyo state, Nigeria.

2. Department of Mechanical Engineering, Faculty of Technology, Obafemi Awolowo University (O.A.U.), Ile-Ife, Osun state, Nigeria.

3. Department of Mechanical Engineering, College of Technology, Federal University of Petroleum Resources, Effurun, P.M.B. 1221, Effurun, Delta state, Nigeria

\*Email of the corresponding author: [pookekunle@lautech.edu.ng](mailto:pookekunle@lautech.edu.ng)

## Abstract

Combined effects of reactor pressure (0.0001, 0.01, 1, 10, 100 atm) and heating rate (10, 20, 30, 40 and 50 K/s) on biomass pyrolysis characteristics at a final reactor temperature of 973 K in thermally thin regime have been numerically investigated. Wood pellets ( $\rho = 400 \text{ kg/m}^3$ ,  $\phi 1 \text{ mm}$  and length  $1 \text{ mm}$ ) were modeled as two-dimensional porous solids. Transport equations, solid mass conservation equations, intra-particle pressure generation equation and energy conservation equation were coupled and simultaneously solved to simulate pyrolysis. Solid mass conservation equations were solved by first order Euler Implicit Method (EIM). Finite Volume Method (FVM) was used to discretize the transport, energy conservation and pressure generation equations, and the resulting linear simultaneous equations were solved by Tri-Diagonal Matrix Algorithm (TDMA). Intra-particle fluid flow velocity was estimated by Darcy's law. Results showed that pressure does not have any significant effect on biomass primary disintegration reactions at all heating rates. Increase in heating rate accelerated the rate of biomass primary conversion. In the vacuum region, increase in pressure did not have any significant effect on tar, gas and secondary tar release rates and yields at all heating rates. Increase in pressure from vacuum to atmospheric, and from atmospheric to pressurized condition diminished tar release rate and yield but favoured gas and secondary tar release rates and yields at all heating rates. Findings further showed that volatiles intra-particle secondary reactions products generation rates at atmospheric and pressurized conditions were ten times and over higher than those at vacuum conditions. It was concluded that at and above atmospheric pressure conditions, pressure can significantly influence the rate of generation, yield and percentage composition of product species.

**Keywords:** Biomass, pyrolysis, pressure, heating rate, intra-particle secondary reactions

## 1. Introduction

The need to go green in energy generation and utilization has been acknowledged the world over. Energy experts have been working tirelessly to see how best the environment can be preserved while at the same time meet energy demands for sustainable development. Biomass energy has become one of the rapidly growing technologies with emphasis on thermochemical conversion methods. A better understanding of various chemical processes and physical phenomena associated with these methods will aid process design and optimization. Pyrolysis, being the precursor of combustion and gasification [1], is an important phase in biomass thermochemical conversion. Many factors influence the rate of pyrolysis, product yields and composition. Heating rate, operating temperature and pressure are the most important. Many researchers have studied the effects of process parameters and other factors affecting biomass pyrolysis [2-14]. Some researchers have reviewed the operating conditions and reactor designs that maximize the yield of char [15, 16] and condensable products [17-20]. Effects of thermo-physical properties on intra-particle secondary reactions have also been investigated [21]. We have studied the effects of pressure on pyrolysis in both thermally thin and thermally thick regimes at a constant heating rate [22, 23]. To the best of authors' knowledge, there has been little research

work done on investigating the simultaneous effect of pressure and heating rate on biomass pyrolysis. This work was therefore undertaken for the purpose of filling this gap.

## 2. Pyrolysis Mechanism

Figure 1 shows the structure of the pyrolysis mechanism adopted in this study. A detailed explanation on the development of this mechanism has been reported in our earlier research works [24, 25]. As shown in the figure, wood first decomposes by three endothermic competing primary reactions to form gas, primary tar and intermediate solid. The primary tar undergoes secondary reactions to yield more gas and char. The intermediate solid is further transformed into char by a strong exothermic reaction as shown in the figure. Reaction rates were assumed to follow Arrhenius expression of the form;  $k_i = A_i \exp\left(\frac{-E_i}{RT}\right)$ . The chemical kinetic ( $A$  and  $E$ ) and thermodynamic ( $a$  and  $b$ ) parameters are as given in one of our previous works [25].

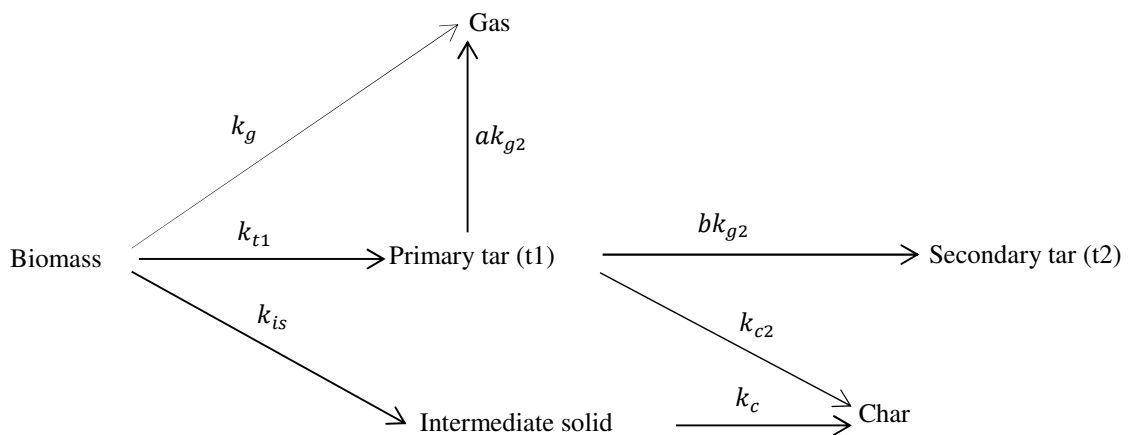


Figure 1: Schematic illustration of pyrolysis mechanism

## 3. Numerical simulation

The governing equations, model assumptions and numerical procedures in this study are already given in our previous studies [24, 25, 21], therefore, fundamental governing equations are only given here.

### 3.1 Solid mass conservation equation

The instantaneous mass balance of the pyrolyzing solid comprises three endothermic consumption terms yielding gas, tar and intermediate solid:

$$\frac{\partial \rho_s}{\partial t} = -(k_g + k_t + k_{is})\rho_s \quad (1)$$

The intermediate solid instantaneous mass balance equation (equation (2)) contains two terms, one for the conversion of the virgin solid to intermediate solid and the other from exothermic decomposition of intermediate solid to yield char, given as

$$\frac{\partial \rho_{is}}{\partial t} = k_{is}\rho_s - k_c\rho_{is} \quad (2)$$

In the same vein, the char instantaneous mass balance equation (equation(3)) contains two terms, one from the exothermic decomposition of intermediate solid and the other from primary tar secondary reaction to yield char, given as

$$\frac{\partial \rho_c}{\partial t} = k_c\rho_{is} + k_{c2}\rho_t \quad (3)$$

### 3.2 Mass conservation equations of gas phase components

Mass conservation equations for all gas phase components are expressed by two-dimensional cylindrical coordinate system consisting of both temporal and spatial gradients and source terms, given by

$$\text{Ar: } \frac{\partial(\varepsilon\rho_{Ar})}{\partial t} + \frac{\partial(\rho_{Ar}U)}{\partial z} + \frac{1}{r} \frac{\partial(r\rho_{Ar}V)}{\partial r} = S_{Ar}, \quad (4)$$

$$\text{Gas: } \frac{\partial(\varepsilon\rho_g)}{\partial t} + \frac{\partial(\rho_gU)}{\partial z} + \frac{1}{r} \frac{\partial(r\rho_gV)}{\partial r} = S_g, \quad (5)$$

$$\text{Primary tar: } \frac{\partial(\varepsilon\rho_{t1})}{\partial t} + \frac{\partial(\rho_{t1}U)}{\partial z} + \frac{1}{r} \frac{\partial(r\rho_{t1}V)}{\partial r} = S_{t1}, \quad (6)$$

$$\text{Secondary tar: } \frac{\partial(\varepsilon\rho_{t2})}{\partial t} + \frac{\partial(\rho_{t2}U)}{\partial z} + \frac{1}{r} \frac{\partial(r\rho_{t2}V)}{\partial r} = S_{t2} \quad (7)$$

$S_{Ar}$ ,  $S_g$ ,  $S_{t1}$  and  $S_{t2}$  are the source terms for the carrier gas (argon), gas, primary tar and secondary tar respectively, and are given by

$$S_{Ar} = 0 \quad (8)$$

$$S_g = k_g\rho_s + \varepsilon k_{g2}\rho_{t1} \quad (9)$$

$$S_{t1} = k_t\rho_s - \varepsilon[k_{c2} + (a + b)k_{g2}]\rho_{t1} \quad (10)$$

$$S_{t2} = \varepsilon b k_{g2}\rho_{t1} \quad (11)$$

Intra-particle tar and gas transport velocity was estimated by Darcy's law,

$$U = -\frac{B}{\mu} \left( \frac{\partial P}{\partial z} \right) \quad (12)$$

$$V = -\frac{B}{\mu} \left( \frac{\partial P}{\partial r} \right) \quad (13)$$

where  $B$  and  $\mu$  are respectively the charring biomass solid permeability and kinematic viscosity. Porosity,  $\varepsilon$ , is expressed as

$$\varepsilon = 1 - \frac{\rho_{s,sum}}{\rho_{w,0}} (1 - \varepsilon_{w,0}) \quad (14)$$

where  $\varepsilon_{w,0}$ ,  $\rho_{s,sum}$  and  $\rho_{w,0}$  are the initial porosity of wood, the sum of solid mass density and initial wood density, respectively. The permeability,  $B$ , of the charring biomass is expressed as a linear interpolation between the solid phase components, given as

$$B = (1 - \eta)B_w + \eta B_c \quad (15)$$

where  $\eta$  is the degree of pyrolysis and is defined as

$$\eta = 1 - \frac{\rho_s + \rho_{is}}{\rho_{w,0}} \quad (16)$$

### 3.3 Energy conservation equation

The energy conservation equation is given as

$$\left( C_{p,w}\rho_s + C_{p,w}\rho_{is} + C_{p,c}\rho_c + \varepsilon C_{p,t}\rho_{t1} + \varepsilon C_{p,t}\rho_{t2} + \varepsilon C_{p,g}\rho_g \right) \frac{\partial T}{\partial t} = \frac{\partial}{\partial z} \left( k_{eff(z)} \frac{\partial T}{\partial z} \right) + \frac{1}{r} \frac{\partial}{\partial r} \left( r k_{eff(r)} \frac{\partial T}{\partial r} \right) - l_c \Delta h_c - \sum_{i=g,t1,is} m_i \Delta h_i - \varepsilon \sum_{i=g2,t2,c2} n_i \Delta h_i \quad (17)$$

where

$$l_c = A_c \exp(-E_c/RT) \rho_{is} \quad (18)$$

$$m_i = A_i \exp(-E_i/RT) \rho_s \quad i = g, t1, is \quad (19)$$

$$n_i = A_i \exp(-E_i/RT) \rho_{t1} \quad i = g2, t2, c2 \quad (20)$$

The thermo-physical properties of the wood sample are as given in our recent study [22].

### 3.4 Pressure evolution

The total pressure is the sum of the partial pressures of the inert gas (argon), gas and secondary tar from the pyrolysis process. It is given as

$$P = P_{Ar} + P_{t2} + P_g; \quad P_i = \frac{\rho_i RT}{M_i} \quad (i = Ar, t2, g) \quad (21)$$

where  $M_i$  and  $R$  are the molecular weight of each gaseous species and universal gas constant, respectively. Combining equations (4), (5), (7), (12), (13) and (21), intra-particle pressure equation was obtained as

$$\frac{\partial}{\partial t} \left( \varepsilon \frac{P}{T} \right) - \frac{\partial}{\partial r} \left[ \frac{BP}{\mu T} \left( \frac{\partial P}{\partial z} \right) \right] - \frac{1}{r} \frac{\partial}{\partial r} \left[ r \frac{BP}{\mu T} \left( \frac{\partial P}{\partial r} \right) \right] = \frac{R}{M_{t2}} S_{t2} + \frac{R}{M_g} S_g \quad (22)$$

### 3.5 Numerical Procedure

Wood pellets were modeled as two-dimensional porous solids. Wood pores were assumed to be initially filled with argon. As the solid was pyrolyzed, tar and gas were formed while argon was displaced to the outer region without participating in the pyrolysis reaction. The solid mass conservation equations (eqs (1) – (3)) were solved by first-order Euler Implicit Method. The mass conservation equations for argon, primary tar, gas and secondary tar (eqs (4) – (7)), energy conservation equation (eq. (17)) and the pressure equation (eq. (22)) were discretized using Finite Volume Method (FVM). Hybrid differencing scheme was adopted for the convective terms. First-order fully implicit scheme was used for the time integral with time step of 0.005 s. The detailed numerical procedure and calculation domain have been given somewhere else [24]. Model assumptions have also been given previously [21].

## 4. Results and discussion

### 4.1 Pressure and heating rate effect on weight fraction history

In order to investigate the impact of different heating rates (10, 20, 30, 40 and 50 K/s) on pyrolysis characteristics in vacuum (0.0001 and 0.01 atm), atmospheric (1 atm) and pressurized (10 and 100 atm) regions, the weight loss history of the sample was simulated. Figures 2 (a) – (e) show the weight loss history of the sample at different heating rates in the three pyrolysis pressure conditions considered. From the figures, it can be seen that for all pyrolysis pressure regions considered (vacuum, atmospheric and pressurized), increase in heating rate accelerated the rate of biomass conversion with the profile for each heating rate being the same at all pressure regions. This is similar to our earlier findings [22]. This implies that increase in pressure within the range considered (0.0001 – 100 atm) does not significantly affect primary degradation of biomass material in thermally thin regime.

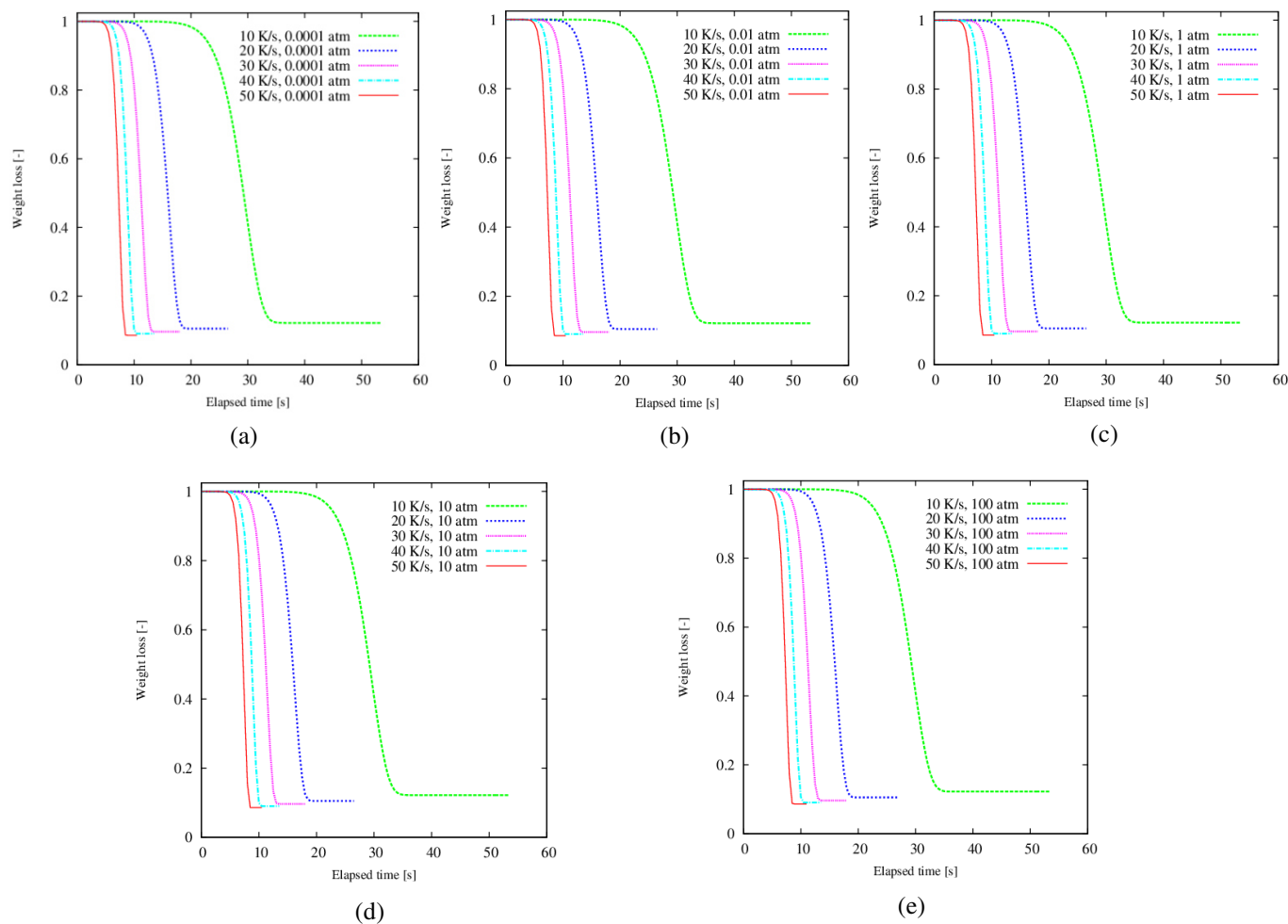


Figure 2: Weight loss history at different reactor pressures and heating rates

#### 4.2 Primary tar production rate

It was of interest to find out the influence of different heating rates on primary tar production rate at vacuum, atmospheric and pressurized pyrolysis conditions. Figures 3 (a) – (e) show the simulated rates of primary tar production at different heating rates for different pyrolysis pressure conditions. From the figure, as would be expected, increase in heating rate accelerated the rate of primary tar production for a given pressure condition. However, primary tar production profile at a particular heating rate was similar for all pyrolysis pressure conditions considered. This result further suggests that increase in pressure does not significantly affect biomass primary decomposition reactions. Other researchers have observed that pressure can influence the yields, compositions, and release rates of gases and liquids in pyrolysis by directly or indirectly affecting volatiles secondary reactions [26]. By implication, pressure influence on pyrolysis is largely due to its effects on volatiles and condensable secondary reactions. This will be further explained in subsequent sections.

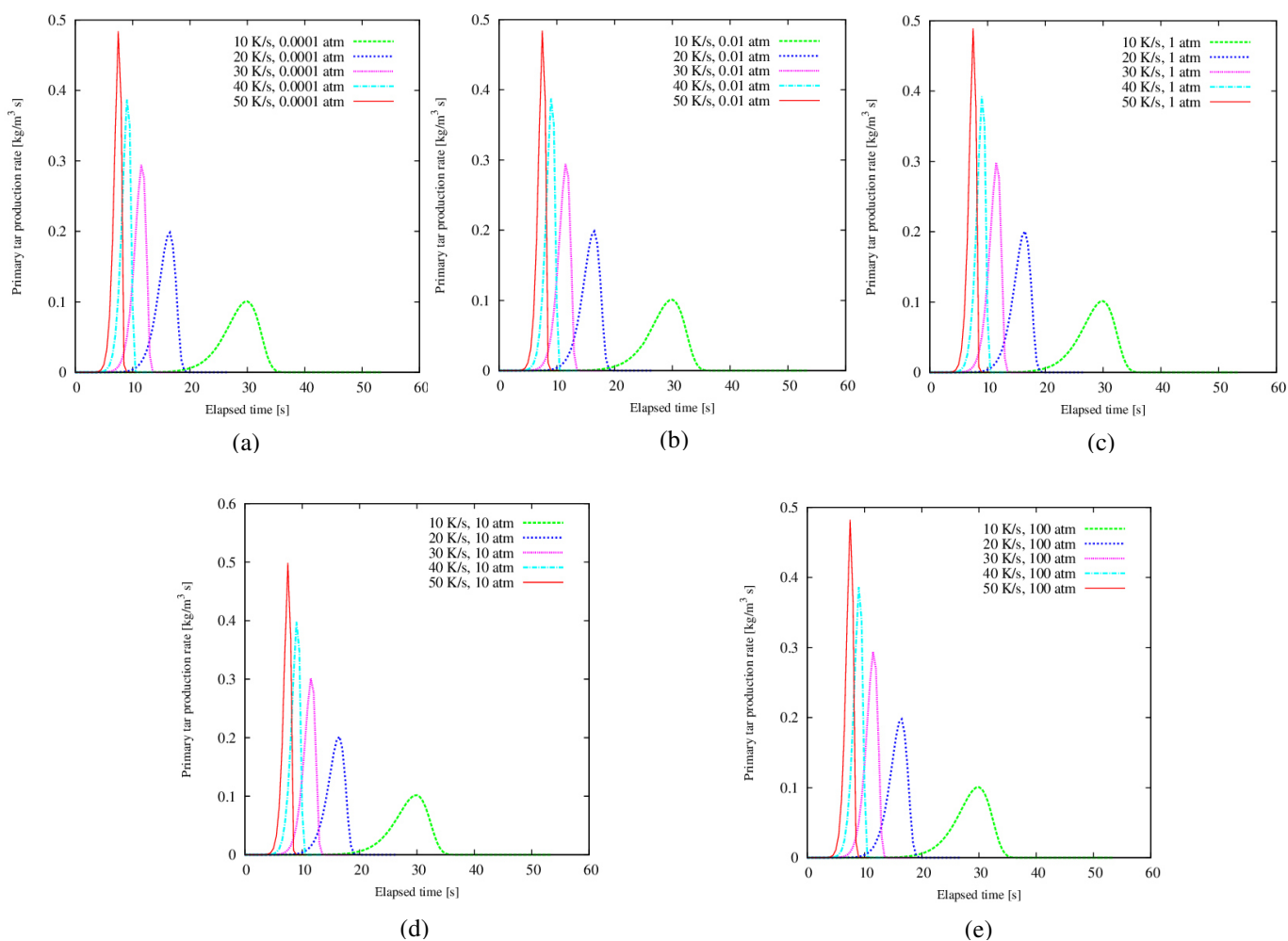


Figure 3: Primary tar production rate at different reactor pressures and heating rates

#### 4.3 Secondary reactions products generation

In order to quantify the extent of primary tar secondary reactions, secondary products generation rate was simulated at different heating rates and different reactor pressure conditions. Figures 4 (a) – (e) show the rate of secondary reactions products generation at various conditions. At 0.0001 atm [Figure 4 (a)], two peaks emerged at all heating rates. The reason for this is not yet clarified and will be a subject of future research. The double peaks scenario however died out with increase in reactor pressure. At vacuum conditions (0.0001 and 0.01 atm), the highest peaks were not at the highest heating rate [Figures 4 (a) and (b)]. This may be due to the subtle nature of volatiles transport and secondary reactions in this region. At atmospheric condition (1 atm), the rate of secondary reactions products generation increased drastically. Furthermore, a closer look at these figures revealed that the rates of generation of secondary reactions products at atmospheric conditions are ten times higher than those at vacuum conditions for all heating rates considered. This can be explained from the standpoint of tar transport and tar secondary reactions. Increase in pressure increased the extent of secondary reactions by slowing down the escape of volatiles from the pyrolyzing sample and its surroundings, thereby making more time available for secondary reactions. A further increase in pressure from atmospheric to pressurized condition (10 atm) resulted in further increase in the rate of generation of secondary reactions

products. However, further increase in pressure within pressurized region (10 to 100 atm) has no significant effect on the rate of generation of these secondary reactions products.

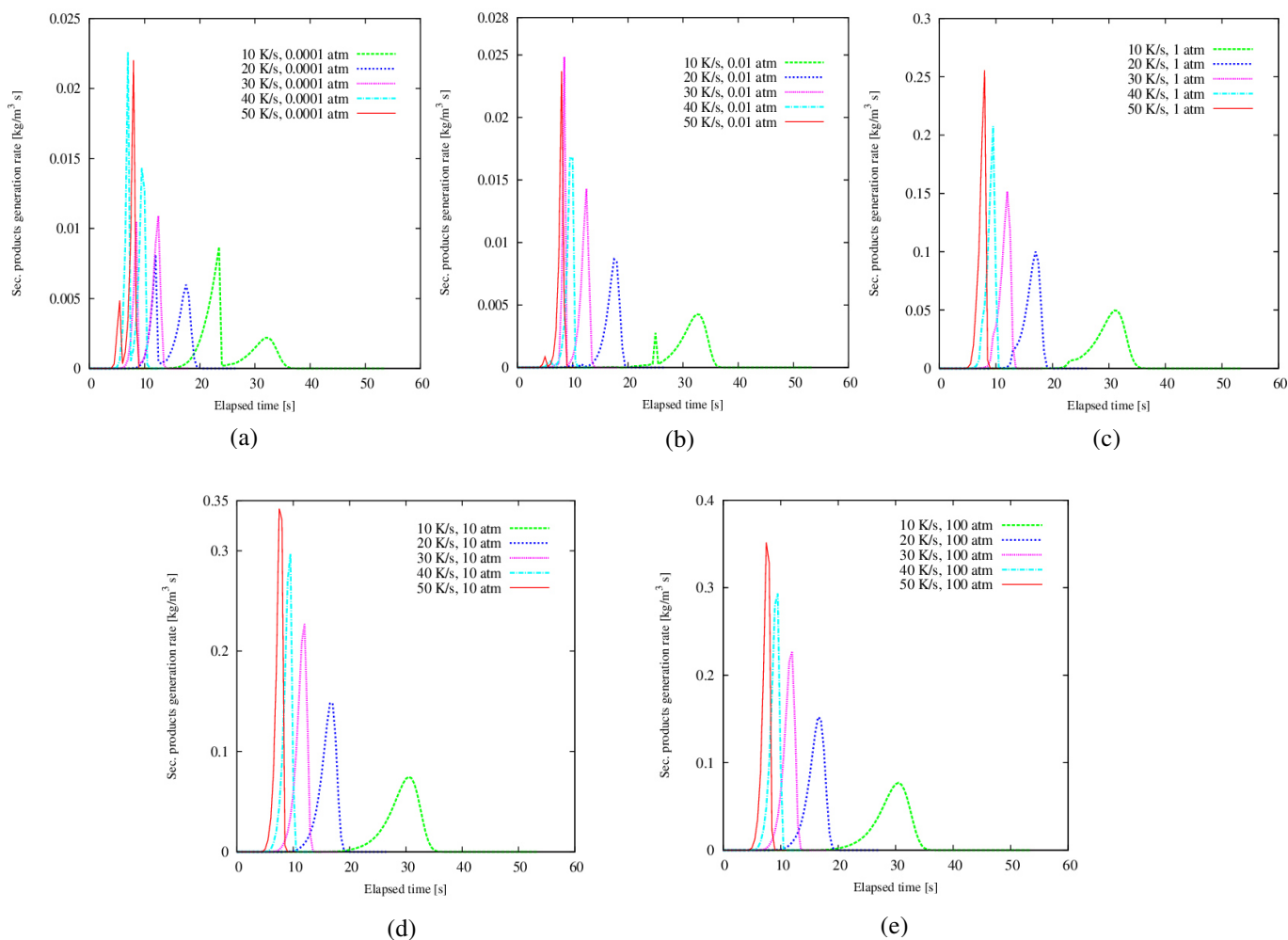


Figure 4: Rate of generation of secondary reactions products

#### 4.4 Tar release rate

Figures 5 (a) – (e) show the rates of tar release at different heating rates and different pressure conditions. From the figures, tar release rate increased with increase in heating rate in all pressure regions while it declined from vacuum to atmospheric and from atmospheric to pressurized region. In the vacuum region, increase in pressure from 0.0001 to 0.01 atm had no significant effect on the rate of tar release at all heating rates [Figure 5 (a) and (b)]. However, as pressure increased from vacuum to atmospheric [Figure 5(b) and (c)], there was reduction in the rate of tar release at all heating rates. As pyrolysis condition changed from atmospheric to pressurized, there was further reduction in the rate of tar release [Figures 5 (c) and (d)]. Moreover, unlike in vacuum region, increase in pressure resulted in further declination in tar release rate [Figure 5 (d) and (e)]. From the pyrolysis mechanism (Figure 1), tar release rate is determined by tar production through biomass primary decomposition reaction and primary tar destruction by secondary reactions. Already, we have observed that pressure does not significantly affect primary disintegration of biomass. Decrease in tar release rate with increasing pressure therefore, as Hajaligol *et al.* [26] reported, must have been due to pressure effects on primary tar transport and secondary reactions. This decrease in tar release rate would no doubt be accompanied with increase in the release rate of gas, char or secondary tar to the degree to which the concerned species is generated by primary tar secondary reactions.

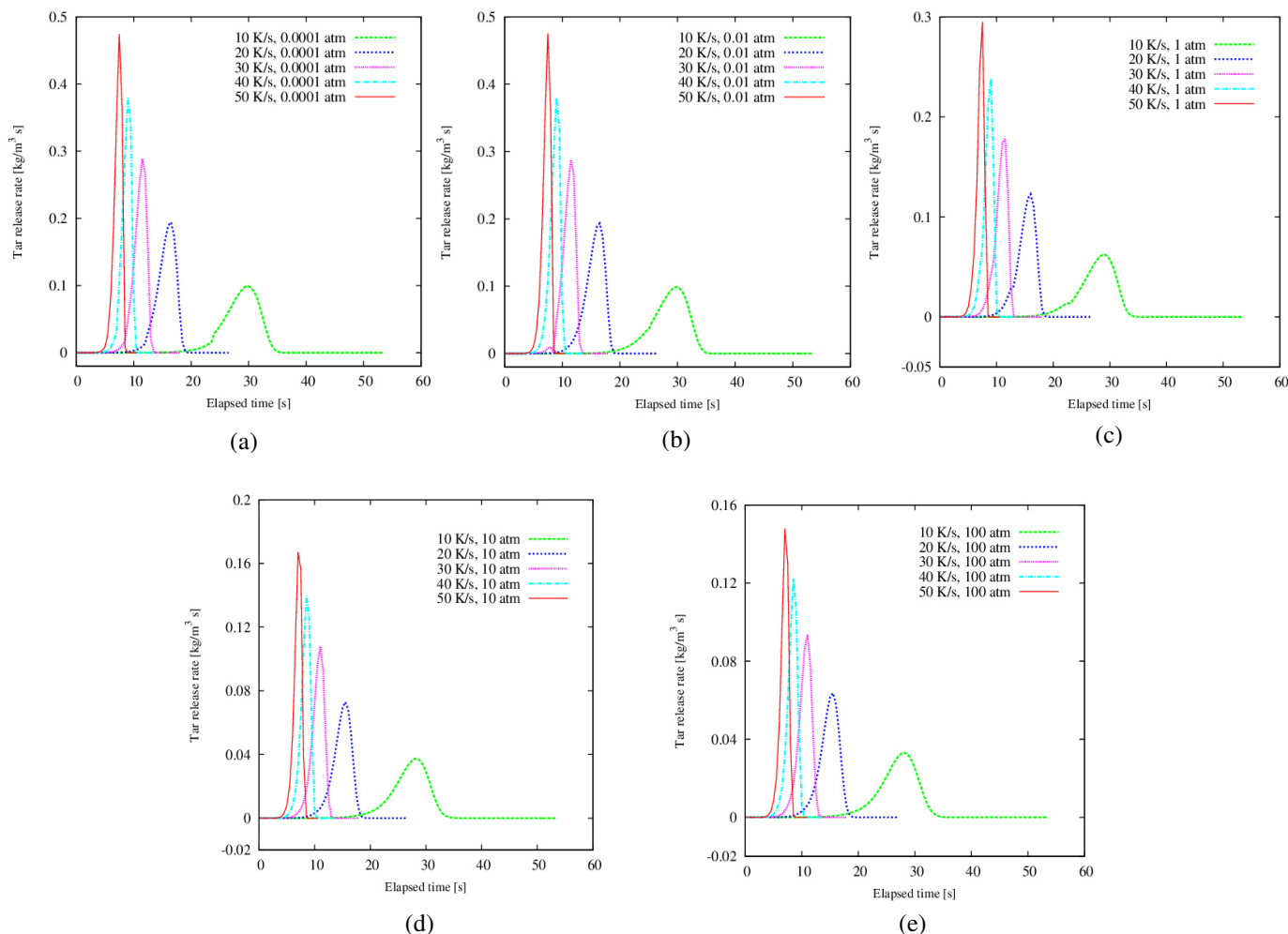


Figure 5: Tar release rate at different reactor pressures and heating rates

#### 4.5 Gas release rate

Figures 6 (a) – (e) show the rate of gas release from the pyrolyzing solid at various pyrolysis pressure regions and at different heating rates. As it would be expected, gas release rate at vacuum, atmospheric and pressurized pyrolysis conditions increased with heating rate. Within the vacuum region, increase in pressure (from 0.0001 to 0.01 atm) did not have any significant effect on gas release rates [Figure 6 (a) and (b)]. As pressure increased from vacuum (0.01 atm) to atmospheric (1 atm), there was increase in gas release rate for all heating rates [Figures 6 (b) and (c)]. As pyrolysis condition changed from atmospheric to pressurized, the rate of gas release was also increased at all heating rates considered [Figure 6 (c) and (d)]. Going by the fact that there was reduction in tar release rate as pressure increased from 10 atm to 100 atm, one would have expected an accompanying increase in gas release rate, especially at 40 K/s and 50 K/s, but there was no noticeable increase in gas release rate in this region. This suggests that either char formation or secondary tar release rate was more favoured in this region. Hajaligol *et al.* [26] reported that char yields above 650 °C increased when pressure was increased from 1.3 to 69 atm. In their research work, they however did not consider the possibility of having secondary tar (assumed to be a mixture of light molecular weight hydrocarbon compounds).



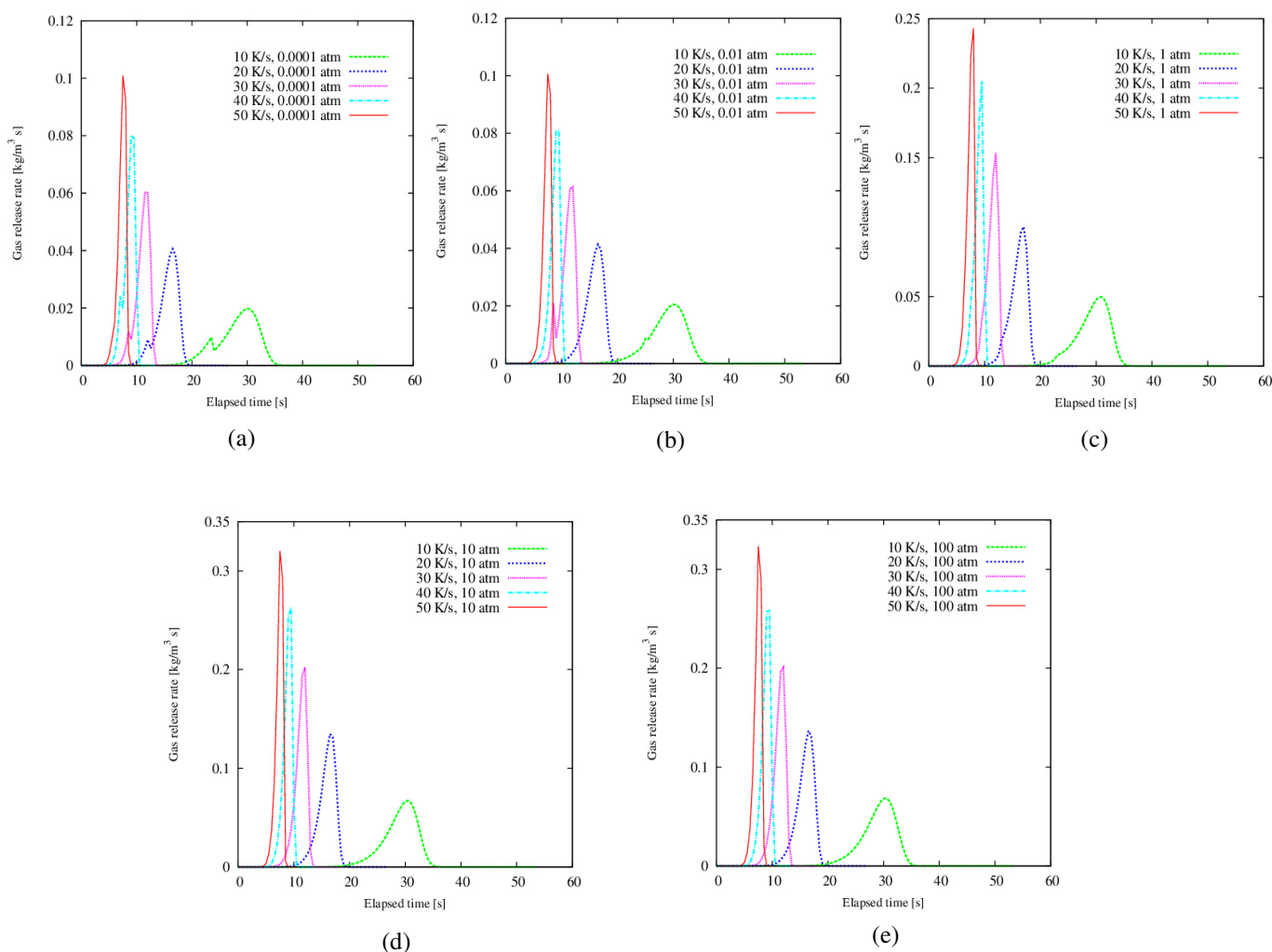


Figure 6: Gas release rate at different reactor pressures and heating rates

#### 4.6 Pressure effect on intra-particle secondary reactions

The extent of the effect of pressure on volatiles (mainly primary tar) intra-particle reactions was analyzed at different pressure regions and heating rates. This was done by finding the ratio of the rate of secondary reactions products generation to the rate of primary tar generation ( $R_s/R_p$ ).  $R_s$  and  $R_p$  have been defined in our previous work [25]. Figure 7 shows the variation of  $R_s/R_p$  for all reactor pressure considered at different heating rates. From the figure, in the vacuum region (0.0001 and 0.01 atm),  $R_s/R_p$  was minimum. This implies that in this region, intra-particle secondary reactions products generation rate was much lower than primary tar generation rate. At low pressure, intra-particle volatiles secondary reactions could not take place appreciably because volatiles transport within and from the pyrolyzing solid was accelerated, making a very short time available for these reactions. This is in agreement with the findings of Hajaligol *et al.* [26]. High tar release rates and yields therefore characterized this region. When pressure increased from vacuum to atmospheric, volatiles residence time within the pyrolyzing sample increased, thereby making more time available for volatiles to undergo intra-particle secondary reactions. This resulted in a drastic increase in the ratio  $R_s/R_p$  (about ten times higher than in vacuum), thereby enhancing the rate of secondary reactions products generation at the expense of tar release rate (Figure 5). When pyrolysis condition changed from atmospheric to pressurized (1 to 10 atm), there was further increase in  $R_s/R_p$ . At this condition, volatiles hold up time within the sample was further increased because their intra-particle transport and their escape from the hot surface were inhibited. This resulted in a higher rate of

generation of secondary reactions products (Figure 4). Further increase in pressure in this region (10 to 100 atm) brought about a little more increase in the ratio  $R_s/R_p$ . From these findings, it is clear that the variation of  $R_s/R_p$  with pressure increase is consistent.

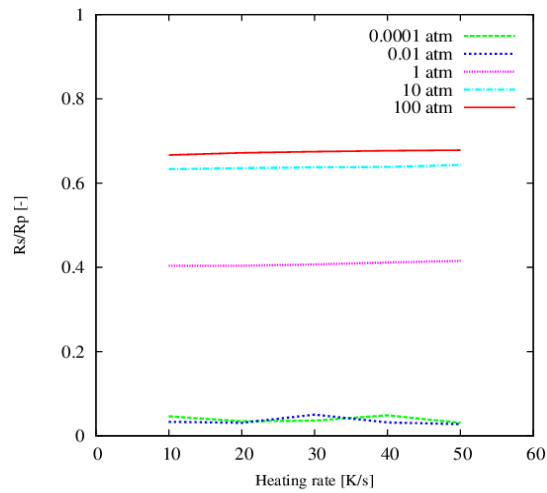


Figure 7: The ratio of the rate of primary tar secondary reactions products generation to the rate of primary tar production at different heating rates

#### 4.7 Final product yields

##### 4.7.1 Total tar yield

Figure 8 shows tar yields at vacuum (0.0001, 0.01 atm), atmospheric (1 atm) and pressurized (10, 100 atm) conditions. The figure shows that maximum tar yields were obtained at vacuum conditions for all heating rates and that there was no significant difference in the tar yield for the two pressure conditions considered in this region. The

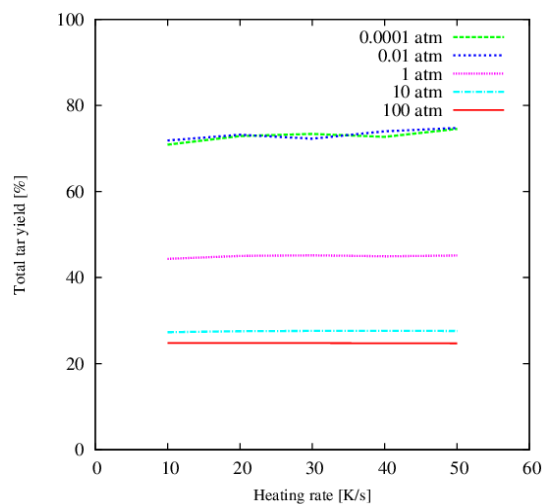


Figure 8: Effects of pressure and heating rate on total tar yield

figure also revealed that pressure effect on product yields is dominant over heating rate effect, as total tar yields were seemingly the same for all heating rates whereas they varied significantly from vacuum to atmospheric and from atmospheric to pressurized condition. Generally, tar yield decreased with pressure increase. These findings suggest that volatiles intra-particle transport and secondary reactions are very sensitive to pressure. Comparison of Figures 7 and 8 clearly reveals that the ratio  $R_s/R_p$  and tar yield are inversely proportional.

#### 4.7.2 Total gas yield

Figure 9 shows the total gas yields for the considered pyrolysis conditions. From the figure, the maximum gas yields were at 100 atm and minimum at 0.0001 and 0.01 atm. Significant increase in gas yield was obtained as pyrolysis condition changed from vacuum to atmospheric, and from atmospheric to pressurized. Within the vacuum region, pressure increase (from 0.0001 to 0.01 atm) did not cause any significant difference in gas yield. This may be due to the fact that transport phenomena and reaction kinetics within this region were almost the same even at different pressure. The same reason may be given to explain the little percentage increase in gas yield observed when pressure increased from 10 to 100 atm in the pressurized region. Going by the rate of gas release at different pressure and heating rates (Figure 6), one would have expected some significant increase in gas yield with increasing heating rate, but from Figure 9, results showed that increase in heating rate did not have so much effect on total gas yield.  $R_s/R_p$  and gas yield are directly proportional.

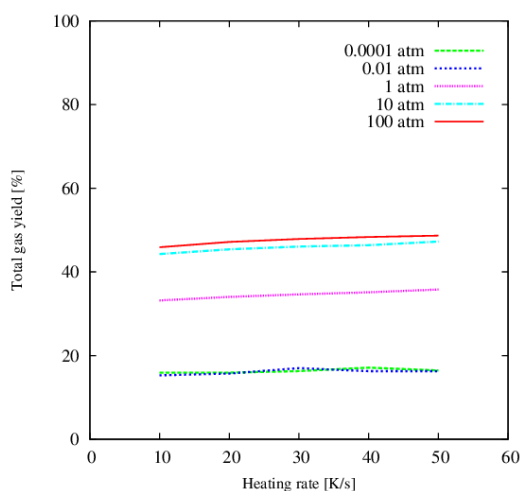


Figure 9: Effects of pressure and heating rate on total gas yield

#### 4.7.3 Total char yield

Figure 10 shows the total char yields at various pyrolysis conditions studied. From the figure, total char yield in all pressure conditions were not significantly different. From weight loss profiles (Figure 2), this kind of result should be expected. This probably may have been due to the fact that thermally thin regime is being considered. Besides, another plausible reason is the fact that extra-particle secondary reactions, which could have made some difference in char yield was not considered in this study.

#### 4.7.4 Secondary tar yield

Figure 11 shows the yield of secondary tar at different pyrolysis pressure and heating rate conditions. From the figure, as in total gas yield, the yield of this species increased as pyrolysis condition changed from vacuum to atmospheric and from atmospheric to pressurized condition. However, the magnitude of increase in this case was much lower than that in gas yield. Also, pressure increase in vacuum region had no noticeable influence on secondary tar yields at all the heating rates considered. Probable explanation for this has been given earlier. This scenario was almost the same in the pressurized region when pressure increased from 10 to 100 atm, except that there was a slight upward shift. Secondary tar is assumed to be light weight hydrocarbon species resulting from volatiles secondary reactions.

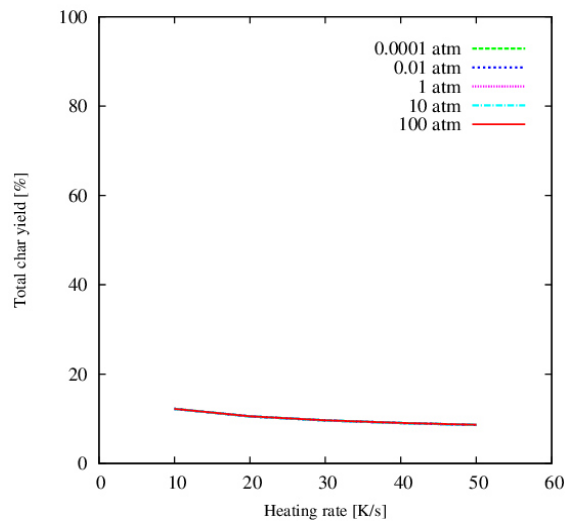


Figure 10: Effects of pressure and heating rate on total char yield

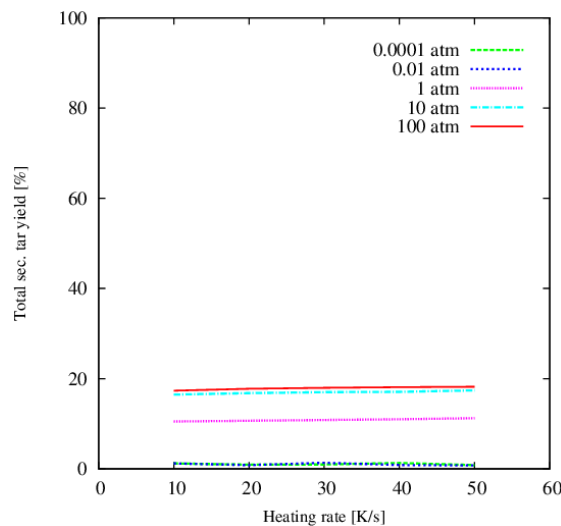


Figure 11: Effects of pressure and heating rate on secondary tar yield

## 5. Conclusions

Combined effects of pressure and heating rate in thermally thin pyrolysis regime have been numerically investigated at vacuum, atmospheric and pressurized conditions. For thermally thin biomass samples, results showed that pressure does not significantly influence biomass primary degradation reactions. Increase in heating rate however accelerated the rate of biomass primary decomposition reactions. In the vacuum region, increase in pressure did not have any significant effect on the rates of products generation and their eventual yields at all heating rates considered (10, 20, 30, 40 and 50 K/s). Pressure increase from vacuum to atmospheric and from atmospheric to pressurized condition resulted in reduction in tar release rate, increase in gas and secondary tar release rates at all heating rates. At vacuum conditions (0.0001 and 0.01 atm), volatiles intra-particle secondary reactions were not significant (very low  $R_s/R_p$ ), the reason these conditions were characterized by high tar release rate and yield. At atmospheric and pressurized conditions, the residence time of volatiles was increased and volatiles intra-particle secondary reactions were significantly enhanced ( $R_s/R_p$  over ten times higher than at vacuum conditions). Char yields were not different in all. Considering extra-particle volatiles secondary

reactions may bring some further insight on char yields. This research will help in pyrolysis process optimization and efficient reactor design.

### Nomenclature

$A$ : pre-exponential factor	(1/s)
$B$ : permeability	( $m^2$ )
$C_p$ : specific heat capacity	(J/ kg K)
$E$ : activation energy	(J/mol)
$e$ : emissivity	(-)
$h_c$ : convective heat transfer coefficient	(W/ $m^2$ K)
$k$ : reaction rate constant	(1/s)
$k_c$ : char thermal conductivity	(W/m K)
$k_w$ : wood thermal conductivity	(W/m K)
$M$ : molecular weight	(kg/mol)
$P$ : Pressure	(Pa)
$Q$ : heat generation	(W/ $m^3$ )
$Q_c$ : convective heat flux	(W/ $m^2$ )
$Q_r$ : radiation heat flux	(W/ $m^2$ )
$R$ : universal gas constant	(J/mol K)
$R$ : total radial length	(m)
$r$ : radial direction	
$z$ : axial direction	
$S$ : source term	
$T$ : temperature	(K)
$t$ : time	(s)
$U$ : axial velocity component	(m/s)
$V$ : radial velocity component	(m/s)
$\varepsilon$ : porosity	(-)
$\varepsilon_0$ : initial porosity	(-)
$\Delta h$ : heat of reaction	(kJ/kg)
$\mu$ : viscosity	(kg/m s)
$\rho$ : density	(kg/ $m^3$ )
$\rho_{w0}$ : initial density of wood	(kg/ $m^3$ )
$\sigma$ : Stefan-Boltzmann constant	(W/ $m^2$ $K^4$ )
$\eta$ : degree of pyrolysis	

### Subscripts

$Ar$ : Argon
$c$ : char, primary char formation reaction
$c_2$ : secondary char formation reaction
$g$ : gas, primary gas formation reaction
$g_2$ : secondary gas formation reaction
$is$ : intermediate solid, intermediate solid formation reaction
$s$ : solid
$t$ : tar, tar formation reaction
$v$ : total volatile
$w$ : wood

### References

- [1] Becidan, M., Skreiberg, Ø. & Hustad, J.E. (2007). Experimental Study on Pyrolysis of Thermally Thick Biomass Residues Samples: Intra-sample Temperature Distribution and Effect of Sample Weight (Scaling Effect). *Fuel*, 86, 2754-2760.
- [2] Lu, H., Ip, E., Scott, J., Foster, P., Vickers, M. & Baxter, L.L. (2010). Effects of Particle Shape and Size on Devolatilization of Biomass particle. *Fuel* 89, 1156-1168.
- [3] Chan, W.R., Kelbon, M. & Krieger, B.B. (1985). Modelling and Experimental Verification of Physical and Chemical Processes during Pyrolysis of a Large Biomass Particle. *Fuel*, 64, 1505-1513.
- [4] Liliedahl, T. & Sjöström, K. (1998). Heat Transfer Controlled Pyrolysis Kinetics of a Biomass Slab, Rod or Sphere. *Biomass and Bioenergy* 15(6), 503-509.

- [5] Fushimi, C., Araki, K., Yamaguchi, Y. & Tsutsumi, A. (2003). Effect of Heating Rate on Steam Gasification of Biomass. 2. Thermogravimetric-Mass Spectrometric (TG-MS) Analysis of Gas Evolution. *Industrial Engineering Chemistry Research*, 42, 3929-3936.
- [6] Papadikis, K., Gu, S. & Bridgwater, A.V. (2009). CFD Modelling of the Fast Pyrolysis of Biomass in Fluidized Bed Reactors. Modeling the Impact of Biomass Shrinkage. *Chemical Engineering Journal* 149, 417-427.
- [7] Bharadwaj, A., Baxter, L.L. & Robinson A.L. (2004). Effects of Intraparticle Heat and Mass Transfer on Biomass Devolatilization: Experimental Results and Model Predictions. *Energy & Fuel* 18, 1021-1031.
- [8] Hage M.J. & Bryden, K.M. (2002). Modeling the Impact of Shrinkage on the Pyrolysis of Dry Biomass. *Chemical Engineering Science*, 57, 2811-2823.
- [9] Park, W.C., Atreya, A. & Baum, H.R. (2010). Experimental and Theoretical Investigation of Heat and Mass Transfer during Wood Pyrolysis. *Combustion and Flame* 157, 481-494.
- [10] Babu, B.V. & Chaurasia, A.S. (2003). Modeling for Pyrolysis of Solid particle: Kinetics and Heat Transfer Effects. *Energy Conversion and Management*, 44, 2251-2275.
- [11] Antal, M.J. (1983). Effects of Reactor Severity on the Gas-phase Pyrolysis of cellulose and Kraft Lignin-derived Volatile Matter. *Industrial Engineering Production Research and Development*, 22, 366-375.
- [12] Scotts, D.S., Piskorz, J., Bergougnou, M.A., Graham, R. & Overend, R.P. (1988). The Role of Temperature in the Fast Pyrolysis of Cellulose and Wood. *Industrial Engineering Chemistry Research* 27, 8-15.
- [13] Pyle, D.L. & Zaror, C.A. (1984). Heat Transfer and Kinetics in the Low Temperature Pyrolysis of Solid. *Chemical Engineering Science*, 19, 147-158.
- [14] Horne, P.A. & Williams, P.T. (1996). Influence of Temperature on the Products from the Flash Pyrolysis of Biomass. *Fuel*, 75, 1051-1059.
- [15] Antal, M.J., Mok, W.S.L., Varhegyi, G. & Szekely T. (1990). Review of Methods for Improving the Yields of Charcoal from Biomass. *Energy & Fuel*, 4, 221-225. In Modeling Chemical and Physical processes of Wood and Biomass Pyrolysis, Progress in Energy and Combustion Science, 34 (2008), 47-90.
- [16] Antal, M.J., Mochidzuki, K. & Paredes, L.S. (2003). Flash carbonization of Biomass. *Industrial Engineering Chemistry Research*, 42, 3690-3696. In Modeling Chemical and Physical processes of Wood and Biomass Pyrolysis, Progress in Energy and Combustion Science, 34 (2008), 47-90.
- [17] Bridgwater A.V. (1999). Principles and Practice of Biomass Pyrolysis Processes for Liquids *Journal of Analytical and Applied Pyrolysis*, 51, 3-22. In Modeling Chemical and Physical processes of Wood and Biomass Pyrolysis, Progress in Energy and Combustion Science, 34 (2008), 47-90.
- [18] Scott, D.S., Majerski, P., Piskorz J. & Radlein, D. (1999). A Second Look at Fast Pyrolysis of Biomass – The RTI Process. *Journal of Analytical and Applied Pyrolysis*, 51, 23-37. In Modeling Chemical and Physical processes of Wood and Biomass Pyrolysis. Progress in Energy and Combustion Science, 34 (2008), 47-90.
- [19] Bridgwater, A.V. & Peacocke, G.V.C. (2000). Fast Pyrolysis Processes for Biomass. *Renewable and Sustainable Energy Reviews*, 4, 1-73. In Modeling Chemical and Physical processes of Wood and Biomass Pyrolysis, Progress in Energy and Combustion Science, 34 (2008), 47-90.
- [20] Bridgwater, A.V. (2003). Renewable Fuels and Chemicals by Thermal processing of Biomass. *Chemical Engineering Journal*, 91, 87-102.
- [21] Okekunle, P.O. (2013). Numerical Investigation of the Effects of Thermo-physical Properties on Tar Intra-particle Secondary Reactions during Biomass Pyrolysis. *Mathematical Theory and Modeling*, 3(14), 83-97.
- [22] Okekunle, P.O. & Osowade E.A. (2014). Numerical Investigation of the Effects of Reactor Pressure on Biomass Pyrolysis in Thermally Thin Regime. *Journal of Chemical and Process Engineering Research*, 27, 12-22.
- [23] Okekunle, P.O., Adeniranye, D.I. & Osowade E.A. (2014). Numerical Investigation of the Effects of Reactor Pressure on Biomass Devolatilization in Thermally Thick Regime. *Journal of Chemical and Process Engineering Research*, 28, 1-8.
- [24] Okekunle, P.O., Watanabe, H., Pattanotai, T. & Okazaki, K. (2012). Effect of Biomass Size and Aspect Ratio on Intra-particle Tar Decomposition during Wood Cylinder Pyrolysis. *Journal of Thermal Science and Technology*, 7(1), 1-15.
- [25] Okekunle, P.O., Pattanotai, T., Watanabe, H. & Okazaki, K. (2011). Numerical and Experimental Investigation of Intra-particle Heat Transfer and Tar Decomposition during Pyrolysis of Wood Biomass. *Journal of Thermal Science and Technology*, 6(3), 360-375.
- [26] Hajaligol, M.R., Howard, J.B. & Peters, W.A. (1993). An Experimental and Modeling Study of Pressure Effects on Tar Release by Rapid Pyrolysis of Cellulose Sheets in a Screen Heater, *Combustion and Flame*, 95, 47-60.